OBLIQUE MJØLNIR MARINE IMPACT: STRUCTURAL AND GEOPHYSICAL DIAGNOSTIC CONSTRAINTS.
F. Tsikalas[1] and J. I. Faleide[2], Department of Geology, University of Oslo, P.O. Box 1047 Blindern, N-0316 Oslo, Norway, [1]filippos.tsikalas@geologi.uio.no, [2]j.i.faleide@geologi.uio.no

The 40-km-diameter Mjølnir crater is a well-established complex marine impact crater in the central Barents Sea [1]. Both geophysical and geological data unequivocally substantiate a meteorite bolide impact at ~142 Ma into an epicontinental basin with 300-500 m paleo-water depth [2, 3].

Obliquity Evidence: It is well documented that the probability for near-vertical and grazing impacts is approximately zero, and that the most probable impact angle of a randomly incident projectile is 45° [4-6]. Following the above estimates, the Mjølnir impact most probably derailed from vertical incidence. In this study, based on the established Mjølnir structure, morphology, and gravity and seismic velocity signatures we search for evidence revealing the impact direction and angle. Such parameters are vital for refining the geographic distribution of ejecta and tsunami-waves, and thus the possible impact-induced regional perturbations and environmental stress.

Elongated crater diameter. The most representative diameter for the near-circular Mjølnir crater was found to be 40 km [7]. We now estimate at 1° intervals the crater diameter around the entire Mjølnir periphery. After normalization to the 40 km average crater diameter, a dominant N-S/NNE-SSW elongation is revealed.

Seismic disturbance asymmetry. For all profiles crossing the center of the structure we have estimated the ratio of the two radii between the crater center and the rim faults. This provides crater radius asymmetry factors and reveals a consistent asymmetry towards the northward direction (NW/N/NE) in the order of ~1.16, ranging 1.33-1.07. The impact-induced seismic disturbance at Mjølnir has a parabolic bowl-shape at the center of the structure and turns into a shallow broad-brim towards the periphery [8]. The crater radius asymmetry is directly translated to a similar asymmetry in the lateral extent of the shallow broad-brim part of the impact-induced disturbance. This part is not only elongated but also slightly shallower in the same northward-direction. Furthermore, the parabolic bowl-shaped disturbance at the crater center is related to the transient cavity and reaches, after decompaction, ~5 km in depth. It appears that the transient cavity maximum depth is offset by 2-2.5 km to the south-southwest relative to the geometric crater center.

Peak-ring character. Although irregular in shape, and varying in width from 1 to 3 km, the raised near-arcuate peak-ring relief bounds the outer perimeter of the annular basin and is delineated by opposite dipping faults with 10-20 m throws. This characteristic shape becomes less clear in the N- and NE-directions where the raised relief is breached and the peak ring remains open, being replaced by faults facing the crater center.

Offsets in brecciation and structural uplift. The residual free-air gravity field exhibits a circular anomaly over the structure (Fig. 1): an annular low, with a 45 km outer diameter attaining minimum values of -1.5 mGal over the periphery, and a central 14-km-wide gravity high, with a maximum value of +2.5 mGal [9]. It appears that the 0-mGal gravity anomaly contour exhibits a distinct SW-NE elongated-shape (Fig. 1). In addition, the annular gravity low (<-0.5 mGal, shaded on Fig. 1), which is directly connected with the region of most intense fracturing and brecciation, closely resembles a horse-shoe shape open to the northeast.

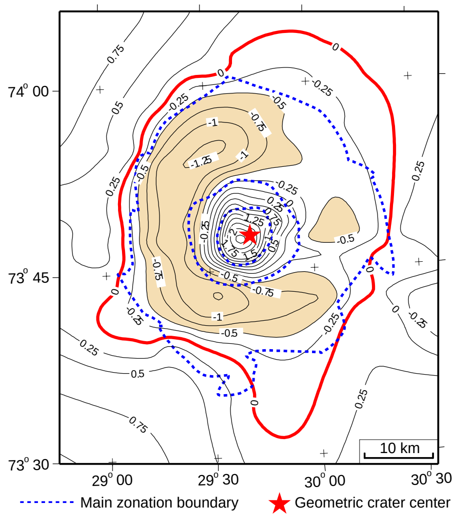

Fig. 1. Residual free-air gravity anomaly map with 0.25 mGal contour interval.

It was estimated that Mjølnir experienced ~1.5-2.0 km of structural uplift [8]. We now show that a north-south seismic reflection profile exhibits a maximum structural uplift lateral offset of 2-2.5 km towards the south from the geometric crater center. Similarly, the gravity central peak which corresponds to the maximum structural uplift [9] is offset by ~1.5-2 km to the southwest from the geometric crater center (Fig. 1). Furthermore, several seismic profiles reveal a small pull-up of the high-amplitude, originally planar Top

Permian reflector beneath the structure. The mapped traveltime anomaly, 16 km in diameter and +80 ms beneath the central crater [9], is slightly offset by ~2 km to the WSW from the geometric crater center.

Impact Direction and Angle: Our analysis has revealed several evidence that, when combined with the established diagnostic structural and geophysical asymmetries of oblique impacts [e.g, 10, 11], can be related to the impact direction and angle. All evidence, including the elongated crater diameter, the crater-radius/seismic-disturbance asymmetry, the peak-ring character, and the offsets in brecciation and structural uplift, clearly point out to a south-southwestern impact direction for Mjølnir. A possible impact angle of ~50°, ranging 30°-60°, is found to be representative for the Mjølnir dimensions based on well-established relationships from laboratory experiments and planetary crater studies [5, 12]. Similar values (impact angle of ~45°, range 30°-60°) were obtained using the Mjølnir crater radius/seismic disturbance asymmetry factors in comparison with laboratory results and numerical computations for oblique impacts at various angles [13, 14].

Nature and Distribution of Proximal Ejecta: An excavated volume of 180-230 km^3 was estimated for Mjølnir [8, 15]. The oblique Mjølnir impact most probably created a down-range sector/corridor of thicker ejecta deposits. Therefore, the ejecta isothickness contours will not probably be circular around the crater site but rather elongated towards the north/northeastern direction (Fig. 2). Recent geochemical analyses at the Mjølnir central crater core have showed absence of siderophile-element anomalies [16]. This translates into low percentage or total absence of projectile material in the crater itself, being consistent with oblique impact models where a large fraction of the projectile material retains a net down-range motion and deposited outside the crater boundaries [17, 18].

Tsunami-waves Distribution: An oblique Mjølnir impact may have generated a down-range elongated water cavity that following its collapse gave rise to faster travelling tsunami-waves at the down-range rather than the up-range region (Fig. 2). The ~80-cm-thick ejecta layer at the borehole 30 km NNE from the crater periphery is the thickest Mjølnir ejecta detected so far. The minor thickness ejecta (≤1 cm) detected on Svalbard and the absence, so far, of tsunami-deposit signatures on NE Greenland, in our view support the obliquity of the Mjølnir impact and possible geographic selectivity in ejecta and tsunami-waves distribution patterns. The proposed model (Fig. 2) envisages thickest ejecta distribution and faster travelling (thus most devastating) tsunami waves concentrated in the area between Svalbard and Novaya Zemlya. Our analysis clearly shows the importance of impact direction and angle in the distribution pattern of ejecta and tsunamis, and further research must, therefore, focus on the proposed down-range region (Fig. 2).

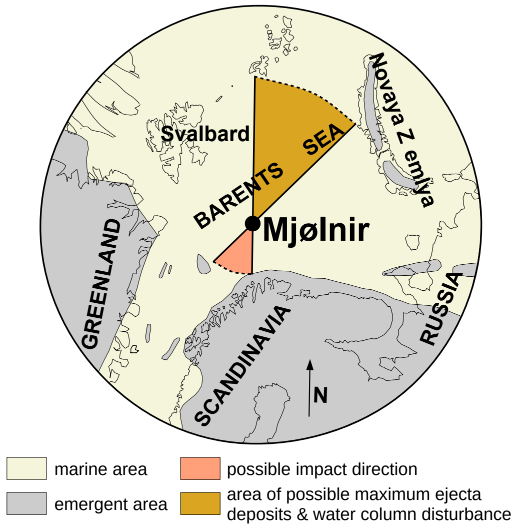

Fig. 2. Mjølnir impact location with possible range of impact direction and down-range area of maximum thickness ejecta and water column disturbance, shown at a ~142 Ma plate reconstruction overlaid on a simplified paleogeographic synthesis.

References: [1] Tsikalas F. et al. (1999) *GSA Special Paper, 339*, 193-204. [2] Smelror M. et al. (2001) *Newsletter on Stratigraphy, 38*, 129-140. [3] Tsikalas F. et al. (2002) *Impact Studies (Impacts in Precambrian Shields), Springer Verlag*, 307-321. [4] Shoemaker E. M. (1962) *Physics and astronomy of the Moon, Acad. Press, New York*, 283-351. [5] Schultz P. H. and Gault D. E. (1990) *GSA Special Paper, 247*, 239-261. [6] Shoemaker E. M. et al. (1990) *GSA Special Paper, 247*, 155-170. [7] Tsikalas F. et al. (1998a) *GSA Bull., 110*, 537-552. [8] Tsikalas F. et al. (1998b) *JGR, 103*, 30469-30484. [9] Tsikalas F. et al. (1998c) *Tectonophysics, 289*, 257-280. [10] Schultz P. H. and Anderson R. R. (1996) *GSA Special Paper 302*, 397-417. [11] Schultz P. H. and D'Hondt S. (1996) *Geology, 24*, 963-967. [12] Schultz P. H. (1992) *JGR, 97*, 16183-16248. [13] Gault D. E. and Wedekind J. A. (1978) *LPS IX*, 3843-3875. [14] O'Keefe J. D. and Ahrens T. J. (1985) *LPS XVI*, 629-630. [15] Shuvalov V. V. et al. (2002) *JGR Planets, 107 (E7)*, 1/1-13. [16] Sandbakken P. (2002) *M.Sc. thesis, Univ. of Oslo*, 142 pp. [17] Schultz P. H. (1996) *JGR, 100*, 21117-21135. [18] Pierazzo E. and Melosh H. J. (2000) *Annual Rev. Earth Plan. Sci., 28*, 141-167.